Publishing House
AKAPIT

COMPUTER METHODS IN MATERIALS SCIENCE

Informatyka w Technologii Materiałów

Vol. 15, 2015, No. 1

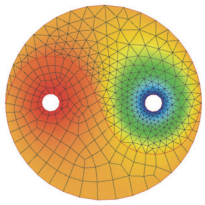

CALCULATION OF FORMING LIMIT CURVE FOR GRADE 2 TITANIUM USING MODIFIED SAMPLE GEOMETRY

JULITA WINOWIECKA*, PIOTR LACKI

Czestochowa University of Technology, Dąbrowskiego 69, 42-202 Czestochowa
**Corresponding author: winowiecka@itm.pcz.pl*

Abstract

Commercially pure titanium Grade 2 has good drawability and tensile strength of about 340 MPa. It is the most widespread grade of titanium in the industry. Grade 2 is characterized by good strength properties, low density, corrosion and external factors resistance. It is widely used in chemical, automotive and aerospace industries. In the aerospace industry titanium Grade 2 is used for production of fuselages, stringers, ventilating ducts, and many other parts. The subject of the work is the forming limit curve (FLC) widely used in industry to determine the possibility of the occurrence of draw-parts defects. FLC is determined based on the relationship between minor and major strains. It is a representation of the limit strains in the plane of the sheets, which in order to avoid cracks, cannot be exceeded during sheet - metal forming.

In the study forming limit curve was determined experimentally and the results were compared with the principal strain calculated in numerical simulations. Numerical simulations of the sheet - metal forming process were prepared in the PamStamp 2G v2012 program, using the finite element method. Forming simulation was carried out for specially designed samples with different lateral cut. The results of experimental studies at a depth corresponding to crack onset were compared with numerical calculations. Distributions of principal strain were determined for all specimens. The minor and major principal strains occurring in the forming samples before rupture onset were analyzed. Based on the results of numerical investigations forming limit curve for the titanium Grade 2 was determined. In experimental studies, in order to determine the plastic deformation ARAMIS system was used that enables non-contact measurements of three-dimensional deformations. The PamStamp 2G program and ARAMIS data acquisition process allowed for analysis of deformation and determination of the values of minor and major principal strains immediately before rupture. The numerical simulations considered technically dry friction and lubrication. This approach allowed for determining the effect of lubrication on strain distributions.

Key words: finite element method, titanium grade 2, forming limit curve

1. INTRODUCTION

Technically pure Grade 2 titanium is the most widespread grade of titanium in the industry. It is characterized by high mechanical strength, low specific gravity, corrosion and external factors resistance. However, titanium materials demonstrate poor suitability to plastic forming using rigid tools at room temperature (Adamus, 2009b). The stamping of Grade 2 titanium elements is connected with the occurrence of return springback, causing shape-dimensional inaccuracies (Winowiecka, 2013; Adamus et al., 2011).

The forming limit curve was developed by Keeler (1965) and Goodwin (1968) in the 1960s, while in the seventies a simplified technique of determining FLC was elaborated (Hecker, 1975). Since that time, FLCs are being continually improved and widely used in the optimization of metal sheet forming processes (Ávila & Vieira, 2003; Butuc et al., 2003; Narayanasamy & Narayanan, 2006, 2008). In 1967, Marciniak and Kuczyński (1967) developed a forming limit curve prediction model based on imperfections in sheet metal. This so -called M-K model has been the most commonly used for analytical prediction of FLC and has been the most crucial for furt her develop-

ISSN 1641-8581

ment of formability assessment in sheet metal forming processes (Banabic, 2010). Marciniak el al. (2002) recapitulated the research on the M-K model and prepared the theory that the forming limit curve allows one to describe local processes of necking and tearing, but it does not depend on the boundary conditions. According to this theory FLC is a material property curve dependent on the strain state. These curves represent the limit strain, where exceedance is associated with drawpiece defects. FLC could be determined in experiment (Dong & Zhang, 2014). Experimentally determined forming limit curves are used in numerical simulations of metal sheet forming (Adamus, 2009a). In the numerical simulations of stamping, FLCs with the Keeler-Goodwin course are also utilized, which are defined based on experimental material properties and sheet thickness (Winowiecka et al., 2013; Winowiecka et al., 2014; Lacki et al., 2013; Adamus & Lacki, 2014).

The ARAMIS system enables two-dimensional and three-dimensional non-contact deformation measurements. Facets with a unique surface structure are applied on the research objects. The cameras make a series of pictures during the process allowing recording of the deformation. Software based on the images analyzes at each step changes in the surface structure. The photos of the two cameras are compared using pixel coordinates in the images. Then the system calculates the displacement of points on the individual images. On this basis it is possible to determine many distributions: the principal strain, thinning or displacement of the three axes. ARAMIS is used for example to measure three-dimensional deformation during stamping and stretching. In addition, the software enables calculation of the forming limit curve for a set of samples based on the minor and major strains (ARAMIS, 2011) .

The use of experimental-numerical methodology is effective to predict the course of forming limit curves. Programs based on the finite element method, e.g. ABAQUS (Djavanroodi & Derogar, 2010) or PamStamp (Oh et al., 2011) are applied to determine the risk of cracks during stamping processes. They allow one to determine the distributions of plastic deformation, principal strain and thinning of the forming drawpiece. Hogström et al. (2009) and Situ et al. (2011) propose the use of the ARAMIS system to determine the experimental strain distribution and ABAQUS program to carry out numerical simulations. Badr et al. (2014) propose the use of optical strain measurement system "Autogrid Vario" to registration of deformation for specimens of various shapes.

2. AIM AND SCOPE OF WORK

The aim of the study was to determine the limit strain for Grade 2 titanium using samples with modified geometry. For the experimental studies, the ARAMIS system allowing non-contact dimensional measurement of deformation was used. Numerical simulations of the forming process of the sample set of square specimens with cuts were conducted using PamStamp 2G v2012, using the finite element method. Sample geometry which allowed appropriate crack location was developed. Square samples were designed with cutouts that fit the dimensions of the stamping tool. In this way cracks at the fillet radii of the die or under the blank holder were avoided. The experimental studies have included applying facets and stamping samples together with the registration process in the ARAMIS system. Numerical simulations were prepared by representing the real tool. The results of the calculations allowed us to determine the distribution of limit strain on the drawpiece surfaces for dry friction conditions and lubrication. By comparing the experimental and numerical results, the principal strain distributions in the drawpiece were analysed.

3. EXPERIMENTAL STUDIES

To determine the forming limit curve, forcing a hemispherical punch in specimens with different geometry was used. Previous studies led to the development of a set of specimens allowing a wider range of deformation. Initially, stamping sheet metal strips with different widths were used. Such samples, however, often cracked in the close vicinity of the blank holder, preventing proper deformation measurement. Using cut-out metal discs, it was possible to obtain easy crack measurement. The cracks frequently initiated near the center of the drawpiece, making easy and accurate measurements possible. In the case of some sample, sliding of the specimen out from under the blank holder caused by too little surface under the blank holder created a problem, therefore, square samples with cutouts were designed. For such a set, the area under the blank holder is the same for all the specimens, and in addition the material does not slide when using low

blank-holder forces. The samples crack near the axis of the sample, according to the assumption.

It was important to design samples adjusted to the dimensions of the real tool, thus reducing the cracks outside the measurement area. A press tool was used with the following dimensions: die hole 34 mm and filleting radius 5 mm, punch with a diameter of 28 mm and pressure ring hole 34 mm. A set of samples with square geometry shown in figure 1 was prepared for forming. The used sample geometry allows deformation differentiation. The resulting principal strain leads to determining FLC the measurement points. Thanks to the various geometries of the sample set, it is possible to vary the stress state using the same tool. The resulting sizes of the main strains are so diverse that it is possible to determine the measurement points on both sides of the ε_2 i $-\varepsilon_2$ axis. The strain paths for different shapes of specimens is shown in figure 2. Used specimens enable realization of stress range from biaxial tension to pure shear.

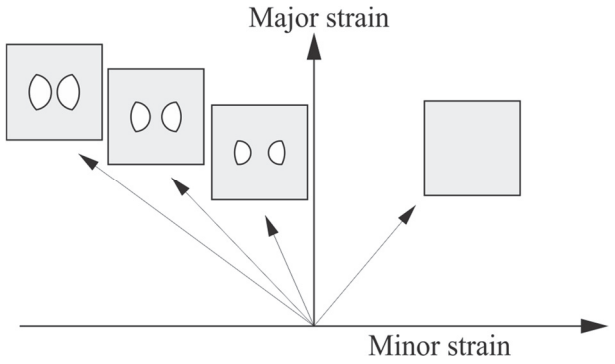

Fig. 2. *The strain paths for different shapes of used specimens.*

4. NUMERICAL STUDIES

A numerical model of the tool was elaborated based on the real tool. The rigid shell model of the tool was prepared using Catia System v.5. The parts of the tool were imported into the PamStamp 2G v2012 program as IGS files. Four-node shell elements were automatically generated on the blank and the tool parts. The boundary conditions were as follows: no degrees of freedom for the die, movement in the Z direction for the punch and the blank-holder, all degrees of freedom for the blank. Additionally, the punch and the blank- holder has a defined displacement, and holding-down force was applied to the blank-holder.

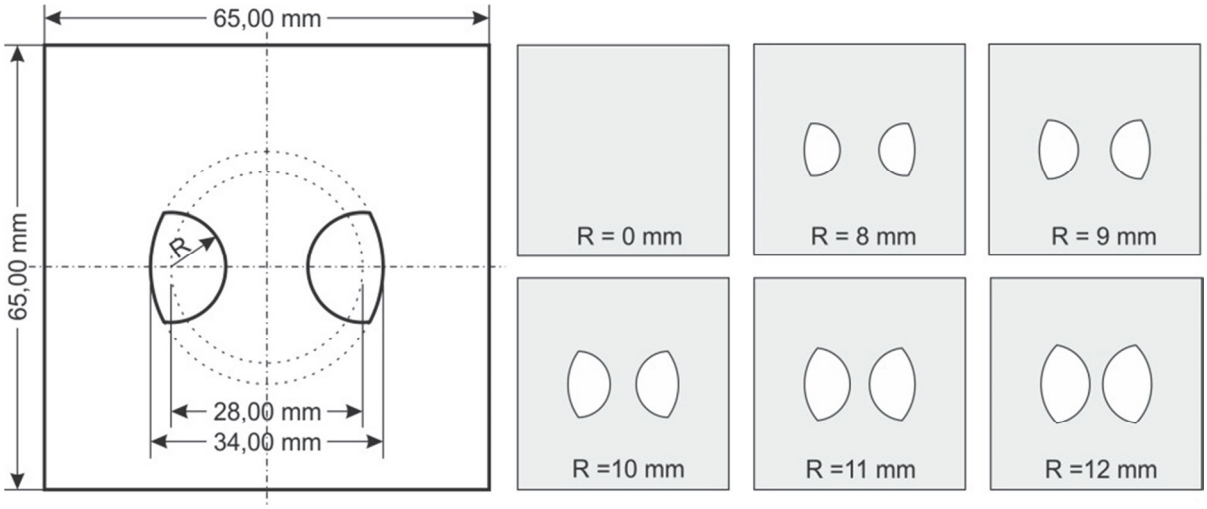

Fig. 1. *Shape and dimension for specimens with cutout.*

Table 1. *Results of experimental studies developed in ARAMIS system.*

Before crack	R = 0 mm	R = 8 mm	R = 9 mm	R = 10 mm	R = 11 mm	R = 12 mm
Height of drawpiece [mm]	14.0	11.2	10.4	9.4	8.7	7.4
Major strain [-]	0.515	0.745	0.684	0.610	0.562	0.553
Minor strain [-]	0.070	-0.482	-0.430	-0.354	-0.330	-0.322

Table 1 shows the values of the minor and major principal strains in the drawpiece and height of the drawpiece. The results enable plotting of the experimental forming limit curve.

The elastic plastic material model was assumed and anisotropic plasticity was used. Hollomon's equation was used to define the relationship between the flow stress and plastic strain. Equation $\sigma = K \cdot \varepsilon^n$ defined the hardening curves of the material. The mechanical properties used for defining the material model are given in table 2.

Table 2. *Material properties used in definition of material model: E – Young's modulus. R_e – yield point. v – Poisson ratio. ρ – specific gravity. K – material constant. n – strain-hardening exponent.*

Property	E GPa	R_e GPa	v -	ρ kg/m^3	K GPa	n -
Grade 2	105	0.236	0.37	4500	0.465	0.125

In the numerical simulations, the following frictional conditions were considered: lubrication μ=0.3 for contact surfaces between the punch and deformed material, μ=0.05 - for the deformed material and blank holder, and deformed material and die, no lubrication - all contact surfaces μ=0.3. The holding-down force was equal to 1.0 kN.

In the experimental studies, the height of the drawn parts at crack moment was measured. The forming process of specimens with lateral cuts was simulated using Finite Element Analysis. The values of major and minor strains were indicated for the same height as the real drawn part at crack.

Figure 3 shows the minor and major principal strain distributions for the analyzed friction conditions for specimens with cutouts with an 8 mm diameter. For specimens for which lubrication was used, the largest major strain obtained is 25% higher in comparison to technical dry conditions. Using the technically dry friction conditions, the largest major strain occurs at the edges of the drawpiece, whereas using lubrication it occurs in the middle. The minor strain in both cases is located at the edges of the cutouts. Using lubrication, the minor strain increased by 40% compared to that obtained without lubrication.

Figure 4 shows the distribution of the major principal strains for the specimen with an R = 9 mm diameter cutout. The distribution of the major principal strains obtained in the numerical simulations is similar to that obtained in experimental studies. The highest values of the major strain occur at the cutout edge in both cases. Figure 4b presents the major strain distribution in the measuring area in the experimental studies. In this case, the maximum value is reached at one of the cutout edges.

The numerical studies have shown differences between the strain values and distribution depending on the friction conditions. Table 3 shows the numerical studies results of the minor and major principal strains obtained for the samples with cutouts. Using lubrication results in a higher value of major strain of 8÷25%, depending on the geometry of the sam-

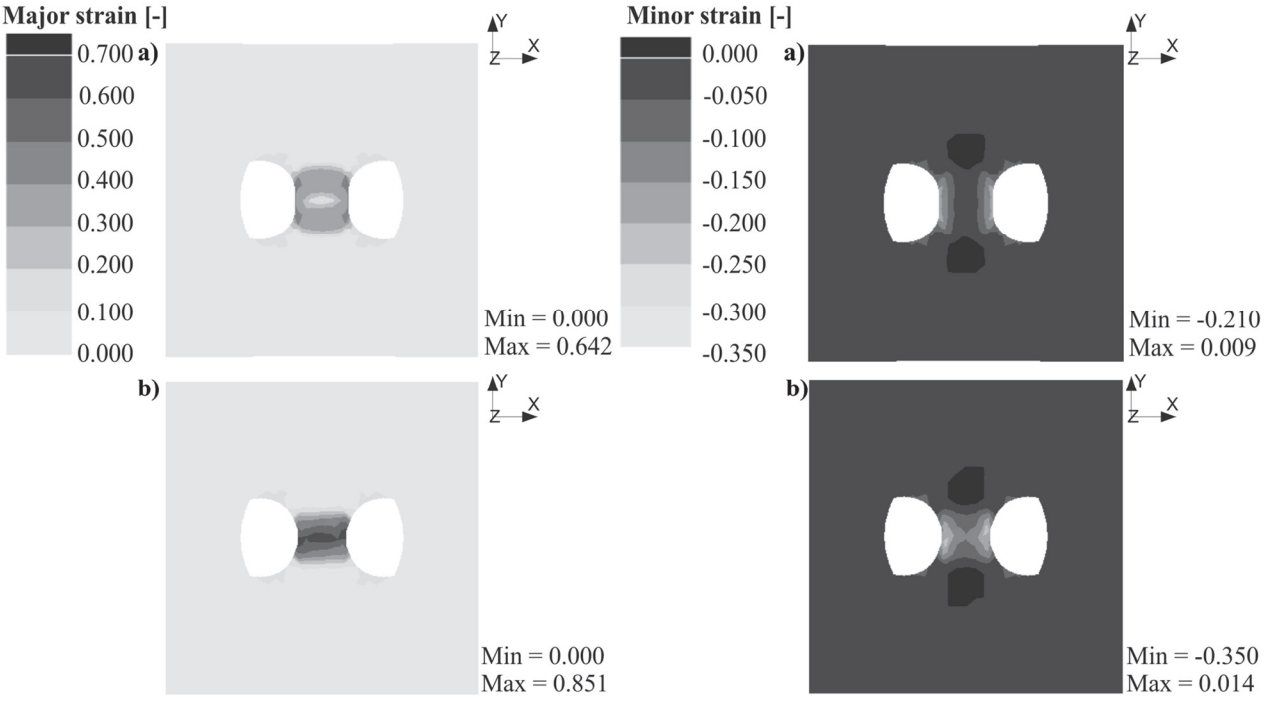

Fig. 3. *Distribution of minor and major principal strains for conditions: dry friction (a), lubrication (b) (R = 8 mm).*

ple, as compared with technically dry friction conditions. Lubrication causes the greatest FLC determined experimentally and numerically. For numerical results the values of major strain are higher than for experimental results.

ing process. This gives a wide range of principal strains. Cracks that prevent correct measurement – under the blank holder or near filleting radius of die, should be avoided. Crack initiation occurs in the middle of the sample.

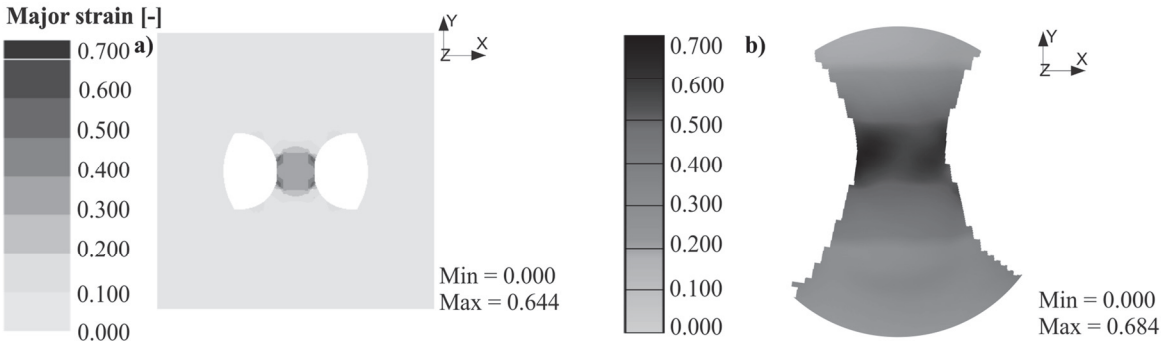

Fig. 4. *Major strain distribution for conditions: dry friction in numerical simulation (a), measurement area in experimental studies(b) (R = 9 mm).*

Table 3. *Results of numerical studies for dry friction and lubrication condition for stamping depth achieved in experimental studies.*

	R=0 mm	*R*=8 mm	*R*=9 mm	*R*=10 mm	*R*=11 mm	*R*=12 mm
	Dry friction condition					
Major strain [-]	0.581	0.642	0.644	0.587	0.591	0.564
Minor strain [-]	0.076	-0.210	-0.260	-0.161	-0.253	-0.239
	Lubrication					
Major strain [-]	0.661	0.851	0.701	0.731	0.778	0.716
Minor strain [-]	0.056	-0.350	-0.273	-0.270	-0.295	-0.259

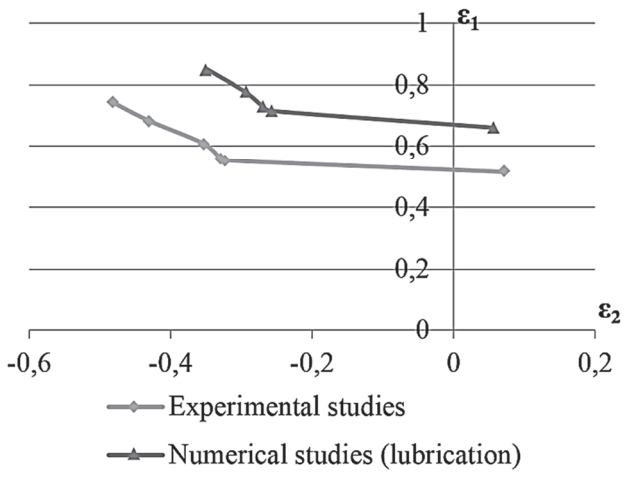

Fig. 5. *FLC for Grade 2 titanium obtained in numerical and experimental studies.*

5. CONCLUSIONS

On the basis of the experimental and numerical studies, the following conclusions can be made:

1. The use of modified square specimen geometry with cutouts allows proper conduct of the forming process. This gives a wide range of principal strains. Cracks that prevent correct measurement – under the blank holder or near filleting radius of die, should be avoided. Crack initiation occurs in the middle of the sample.
2. It is possible to determine the values of the principal strain using experimental-numerical methodology. The numerical process supporting the contactless strain measurement system allows for precise determination of the minor and major strains in the process of stamping specimens with different geometries.
3. The use of dry friction conditions reduces the depth of stamping and principal strain compared to lubrication conditions . Assuming the friction coefficient corresponding to lubrication, at least an 8% increase in the value of major strain was received.
4. Crack initiation with tool lubrication takes place in the middle of the area, compared with crack initiation near the cutout in dry friction conditions.

ACKNOWLEDGEMENT

Financial support of Structural Funds in the Operational Programme – Innovative Economy (IE OP)

financed from the European Regional Development Fund - Project "Modern material technologies in aerospace industry", Nr POIG.01.01.02-00-015/08-00 is gratefully acknowledged.

REFERENCES

ARAMIS, 2009, *ARAMIS, ARGUS, SVIEW - FLC Computation v6.1.1 and higher*.

ARAMIS, 2011, *ARAMIS v6.3 and higher - User Manual*.

Adamus, J., 2009a, Theoretical and Experimental Analysis of the Sheet-Titanium Forming Process, *Arch Metall Mater*, 54, 705-709.

Adamus, J., 2009b, Titanium and its Alloys as a Material Used for the Drawn-Parts, *Inżynieria Materiałowa*, 30, 310-313.

Adamus, J.,Lacki, P., 2014, Analysis of Forming Titanium Welded Blanks, *Computational Materials Science*, 94, 66-72.

Adamus, J., Lacki, P., Łyźniak, J.,Motyka, M., 2011, Optimization of the Stamping Process of A Deflector Element Made of Titanium Grade 2, *Rudy i Metale Nieżelazne*, 56, 588-593.

Ávila, A.F.,Vieira, E.L.S., 2003, Proposing a Better Forming Limit Diagram Prediction: A Comparative Study, *J Mater Process Tech*, 141,101-108.

Badr, O.M., Rolfe, B., Hodgson, P., Weiss, M., 2014, Forming of High Strength Titanium Sheet at Room Temperature, *Mater Design*, in press.

Banabic, D., 2010, A Review on Recent Developments of Marciniak-Kuczyński Model, *Computer Methods in Materials Science*, 10, 225-237.

Butuc, M. C., Gracio, J. J., Barata da Rocha, A., 2003, A Theoretical Study on Forming Limit Diagrams Prediction, *J Mater Process Tech*, 142, 714-724.

Djavanroodi, F.,Derogar, A., 2010, Experimental and Numerical Evaluation of Forming Limit Diagram for Ti6Al4V Titanium and Al6061-T6 Aluminum Alloys Sheets, *Mater Design*, 31, 4866-4875.

Dong, W.-Q., Zhang, X.-L., 2014, Experimental Study on the Forming Limit Diagrams (FLD) of Aerospace Sheet Metal Materials, *Journal of Plasticity Engineering*, 21, 41-45.

Goodwin, G. M., 1968, Application of Strain Analysis to Sheet Metal Forming Problems in the Press Shop, *Metall Italiana*, 60, 764-774.

Hecker, S. S., 1975, Simple Technique for Determining Forming Limit Curves, *Sheet Metal Industry*, 53, 671–675.

Hogström, P., Ringsberg, J. W.,Johnson, E., 2009, An Experimental and Numerical Study of the Effects of Length Scale and Strain State on the Necking and Fracture Behaviours in Sheet Metals, *Int J Impact Eng*, 36, 1194–1203.

Keeler, S. P., 1965, Determination of Forming Limits in Automotive Stampings, *Sheet Metal Industry*, 42, 683-691.

Lacki, P., Adamus, J., Więckowski, W.,Winowiecka, J., 2013, Evaluation of Drawability of Titanium Welded Sheets, *Arch Metall Mater*, 58, 139-143.

Marciniak, Z., Kuczyński, K., 1967, Limit Strains in the Process of Stretch-Forming Sheet Metal, *Int J Mech Sci*, 9, 609-620.

Marciniak, Z., Duncan, J.L. and Hu, S.J., 2002, *Mechanics of Sheet Metal Forming, Butterworth-Heinemann*, London.

Narayanasamy, R., Narayanan, C. Sathiya, 2006, Forming Limit Diagram for Indian Interstitial Free Steels, *Mater Design*, 27, 882–899.

Narayanasamy, R., Narayanan, C. Sathiya, 2008, Forming, Fracture and Wrinkling Limit Diagram for IF Steel Sheets of Different Thickness, *Mater Design*, 29, 1467-1475.

Oh, K. S., Oh, K. H., Jang, J. H., Kim, D. J. ,Han, K. S., 2011, Design and Analysis of New Test Method for Evaluation of Sheet Metal Formability, *J Mater Process Tech*, 211, 695-707.

Situ, Q., Jain, M. K., Metzger, D. R., 2011, Determination of Forming Limit Diagrams of Sheet Materials with a Hybrid Experimental–Numerical Approach, *Int J Mech Sci*, 53, 707-719.

Winowiecka, J., 2013, The Analysis of Springback of Titanium Sheet after Bending, *Obróbka Plastyczna Metali*, 24, 219-231.

Winowiecka, J., Więckowski, W., Lacki, P., Adamus, J., 2014, Numeryczno-Doświadczalna Analiza Procesu Tłoczenia Spawanych Blach Tytanowych, *Rudy i Metale Nieżelazne*, 59, 173-181.

Winowiecka, J., Więckowski, W., Zawadzki, M., 2013, Evaluation of Drawability of Tailor-Welded Blanks Made of Titanium Alloys Grade 2 || Grade 5, *Comp Mater Sci*, 77, 108-113.

WYZNACZANIE KRZYWEJ ODKSZTAŁCEŃ GRANICZNYCH DLA TYTANU GRADE 2 PRZY WYKORZYSTANIU ZMODYFIKOWANEJ GEOMETRII PRÓBEK

Streszczenie

Technicznie czysty tytan Grade 2 charakteryzuje się dobrą tłocznością i granicą wytrzymałością ok. 340 MPa. Jest najbardziej rozpowszechnionym gatunkiem tytanu w przemyśle. Grade 2 cechuje się dobrymi właściwościami wytrzymałościowymi, małą gęstością, odpornością na korozję i czynniki zewnętrzne. Powszechnie wykorzystywany jest w przemysłach chemicznym, motoryzacyjnym i lotniczym. W przemyśle lotniczym z tytanu Grade 2 wykonuje się między innymi elementy kadłubów, wsporniki, kanały wentylacyjne. Przedmiotem pracy jest wyznaczenie krzywej odkształceń granicznych (KOG), stosowanej powszechnie w przemyśle do określania możliwości wystąpienia wad wytłoczek. KOG wyznacza się w oparciu o zależność pomiędzy odkształceniami głównymi najmniejszymi i największymi. Jest to reprezentacja odkształceń głównych w płaszczyźnie blach, które aby uniknąć pęknięć wytłoczki nie mogą być przekroczone w trakcie kształtowania.

W pracy wyznaczano krzywą odkształceń granicznych stosując badania doświadczalne a wyniki odkształceń głównych odniesiono do symulacji numerycznych. Symulacje numeryczne procesu tłoczenia przygotowano w programie PamStamp 2G v2012, wykorzystującego metodę elementów skończonych. Symulację tłoczenia przeprowadzono dla specjalnie zaprojektowanych próbek o różnych wycięciach. Wyniki tłoczenia z badań doświadczalnych przy głębokości tłoczenia dla której uzyskano pęknięcie porównano z obliczeniami numerycznymi. Dla wszystkich próbek wyznaczano rozkłady odkształceń głównych. Analizowano odkształcenia główne największe i najmniejsze występujące w tłoczonych próbkach przed pęknięciem. W oparciu o rezultaty badań numerycznych wyznaczono krzywą odkształceń granicz-

nych dla tytanu Grade 2. W badaniach doświadczalnych do określenia odkształceń plastycznych zastosowano system ARAMIS, umożliwiający bezkontaktowy trójwymiarowy pomiar odkształceń. Program PamStamp 2G oraz rejestracja procesu w systemie ARAMIS pozwoliły na analizę deformacji i wyznaczenie wielkości odkształceń głównych bezpośrednio przed pęknięciem. W symulacjach numerycznych rozważano tarcie technicznie suche oraz smarowanie. Dzięki temu było również możliwe określenie wpływu smarowania na rozkłady odkształceń.

Received: September 30, 2014
Received in a revised form: December 22, 2014
Accepted: December 2, 2014